Exciton-Phonon Information Flow in the Energy Transfer Process of Photosynthetic Complexes

Exciton-phonon information flow in the energy transfer process of photosynthetic complexes

Patrick Rebentrost[1,*] and Alán Aspuru-Guzik[1,†]

[1]*Department of Chemistry and Chemical Biology, Harvard University, 12 Oxford St., Cambridge, MA 02138*

(Dated: November 17, 2010)

Non-Markovian and non-equilibrium phonon effects are believed to be key ingredients in the energy transfer in photosynthetic complexes, especially in complexes which exhibit a regime of intermediate exciton-phonon coupling. In this work, we harness a recently developed measure for non-Markovianity to elucidate the information flow between electronic and vibrational degrees of freedom. We study the measure in the hierarchical equation of motion approach which captures strong system-bath coupling effects and non-equilibrium molecular reorganization. We find that, for a model dimer system and the Fenna-Matthews-Olson complex, non-Markovianity is significant under realistic physiological conditions. A first step towards experimental quantification is provided by the study of four-wave mixing initial states.

The initial step in photosynthesis involves highly efficient excitonic transport of the energy captured from photons to a reaction center [1]. In most higher plants and other organisms such as green sulphur and purple bacteria this process occurs in light-harvesting complexes which are electronically coupled chlorophyll molecules embedded in a solvent and a protein environment [2]. Several recent experiments show that excitonic coherence can persist for several hundreds of femtoseconds even at physiological temperature [3–6]. These experiments suggest the hypothesis that quantum coherence may be biologically relevant for photosynthesis. The results have motivated a sizeable amount of recent theoretical work regarding the reasons for the long-lived coherences and their role to the function. It was shown that the transport efficiency is enhanced by the interplay of the excitonic dynamics with the vibrational environment [7–11]. Employing entanglement measures, defined in the site basis, can lead to further insights [12–14].

The challenging regime of intermediate coupling of the electronic to the vibrational degrees of freedom motivates the study of sophisticated master equations with non-Markovian effects. Several approaches have been taken, ranging from a polaron transformation [15], quantum state diffusion [16], non-Markovian quantum jumps [17, 18], quantum path integrals (QUAPI) [19], to density matrix renormalization group (DMRG) [20]. After photoexcitation, the nuclear coordinates of a molecule will relax to new equilibrium positions, a phenomenon that is borne out by the time-dependent Stokes shift, that is the frequency shift between absorption and emission spectra. Redfield theory assumes that the phonon bath is always in thermal equilibrium and thus cannot capture this effect [21]. Ishizaki and Fleming employed the hierarchical equation of motion (HEOM) approach [22, 23], which interpolates between the usual weak and strong (singular) exciton-phonon coupling limits and takes into account non-equilibrium molecular reorganization effects.

In this work, we study the non-Markovianity of the exciton transfer process by means of numerical simulation. Quantum mechanical time evolution under decoherence leads to transfer of information encoded in the electronic excited state to the vibrational degrees of freedom. In this context, non-Markovianity can be characterized as the return of information to the electronic degrees of freedom. To quantify this information flow, we employ the state-of-the art master equation approach by Ishizaki and Fleming and a newly developed measure for non-Markovianity. The central question we will answer is how much information is exchanged between excitonic and phononic degrees of freedom in that process and, specifically, how much information returns from the phonons to the exciton. Additionally, we provide a step towards the experimental characterization of this effect by investigating the preparation of optimal initial states.

Measure for non-Markovianity– A recent area of research is the study of measures to characterize non-Markovianity [24–27]. We utilize the readily applicable measure developed by Breuer and co-workers [25]. It is based on the quantum state trace distance:

$$D\left(\rho_1\left(t\right),\rho_2\left(t\right)\right)=\frac{1}{2}\mathrm{Tr}\left\{\left|\rho_1\left(t\right)-\rho_2\left(t\right)\right|\right\}, \qquad (1)$$

where $|A|=\sqrt{A^\dagger A}$. This measure quantifies the distinguishablility of two quantum states ρ_1 and ρ_2. For a completely positive trace-preserving map E the trace distance is contractive, i.e. $D\left(E\left(\rho_1\right),E\left(\rho_2\right)\right)\leq D\left(\rho_1,\rho_2\right)$ [28]. Time intervals in which D increases indicate non-Markovian information flow [25], in our case from the vibrational degrees of freedom back to the electronic degrees of freedom. In terms of the slope of D, i.e. $\sigma\left(\rho_1\left(t\right),\rho_2\left(t\right)\right)=\frac{d}{dt}D\left(\rho_1\left(t\right),\rho_2\left(t\right)\right)$, this implies that $\sigma>0$ for these time intervals. Formally, a measure for non-Markovianity is defined by the following [25]:

$$\text{NM-ity}=\max_{\rho_1(0),\rho_2(0)}\int_0^\infty dt\,\alpha\left(\sigma\left(t\right)\right)\,\sigma\left(\rho_1\left(t\right),\rho_2\left(t\right)\right). \qquad (2)$$

Here, $\alpha\left(x>0\right)=1$ $\left(\alpha\left(x<0\right)=0\right)$, to only monitor an increasing trace distance i.e. information backflow. The optimization of the initial states in Eq. (2) obtains the maximally possible non-Markovianity of a particular quantum evolution. In the case of photosynthetic energy transfer, initial states are given by the particular physical situation and lead to smaller values for the non-Markovianity. We use both physical and optimized initial states in this work.

Hierarchy equation of motion– The Hamiltonian describing a single exciton in a complex with N molecules is given

by:

$$H_e = \sum_m^N (\epsilon_m + \lambda)|m\rangle\langle m| + \sum_{m<n} J_{mn}\left(|m\rangle\langle n| + |n\rangle\langle m|\right), \tag{3}$$

where the site energies ϵ_m, and couplings J_{mn} are obtained from detailed quantum chemistry studies and/or fitting of experimental data. The set of states $|m\rangle$ denotes the site basis. The reorganization energy λ is the energy difference of the non-equilibrium phonon state after Franck-Condon excitation and the equilibrium phonon state and is assumed to be the same for each site. The superoperator corresponding to H_e is $\mathcal{L}_e\rho = [H_e, \rho]$. The Hamiltonian for the phonon environment is $H_{ph} = \sum_i \hbar\omega_i \left(p_i^2 + q_i^2\right)$, where ω_i, p_i, and q_i are the frequency, dimensionless momentum and position operators of the phonon mode i. The coupling of the electronic degrees of freedom to the phonons is given by the Hamiltonian $H_{ex-ph} = \sum_m V_m \left(\sum_i g_i q_i\right)_m$, with $V_m = |m\rangle\langle m|$ and where we assume that site-energy fluctuations dominate, the bath degrees of freedom at each site are uncorrelated, and the coupling constants to the respective modes are given by the constants g_i. The spectral density, which describes the coupling strength of exciton to particular phonon modes, is given by $J(\omega) = 2\lambda\gamma\omega/\left(\omega^2 + \gamma^2\right)$. Perhaps the most relevant parameter, the bath dissipation rate γ, is related to the bath correlation time by $\tau_c = 1/\gamma$. The open systems dynamics of the exciton is described by an equation of motion for the reduced excitonic density matrix ρ. It can be obtained by tracing out the less relevant phonon degrees of freedom and utilizing Wick's theorem for the Gaussian fluctuations. The resulting non-perturbative equation of motion can be expressed as a hierarchy of system and auxilliary density operators (ADOs):

$$\begin{aligned}\frac{\partial}{\partial t}\sigma^{\mathbf{n}}(t) &= -\left(i\mathcal{L}_e + \sum_i n_i\gamma\right)\sigma^{\mathbf{n}}(t) \\ &\quad + \sum_i \phi_i\sigma^{\mathbf{n}_{i+1}}(t) + \sum_i n_i\theta_i\sigma^{\mathbf{n}_{i-1}}(t).\end{aligned} \tag{4}$$

The system density matrix is the first member of the hierarchy $\rho(t) = \sigma^{\mathbf{0}}(t)$. The other members of the hierarchy are arranged in tiers and indexed by $n = (n_1, ..., n_N)$, with the notation $\mathbf{n}_{j\pm1} = (n_1, ..., n_j \pm 1, ..., n_N)$. The superoperators in the high temperature regime $\hbar\gamma\beta < 1$ are $\phi_i\sigma^{\mathbf{n}} = i\left[V_i, \sigma^{\mathbf{n}}\right]$ and $\theta_i\sigma^{\mathbf{n}} = i\left(2\lambda/\beta\hbar^2\left[V_i, \sigma^{\mathbf{n}}\right] - i\lambda\gamma/\hbar\left\{V_i, \sigma^{\mathbf{n}}\right\}\right)$ and act on system and ADOs, where $\{,\}$ is the anticommutator. Initially, all the hierarchy members are zero, which corresponds to the electronic ground state phonon equilibrium configuration. For numerical propagation, the hierarchy is truncated based on the criterion $\sum_i n_i \gg \frac{\omega_c}{\gamma}$. We assume that this condition is satisfied when the $\sum_i n_i$ is by a factor 5 larger than $\frac{\omega_c}{\gamma}$.

Results for a dimer– In this section, a two-molecule system, or dimer, is studied in terms of the measure for non-Markovianity using the hierarchy equation of motion approach and scanning over the parameters of the model. As standard parameters, we use the site energies $\epsilon_1 = 0$, $\epsilon_2 = 120/\mathrm{cm}$, and the coupling $J = -87.7/\mathrm{cm}$. This corresponds to the strongly-coupled bacteriochlorophyll site 1 and 2 subsystem of the Fenna-Matthews-Olson complex. For the molecular reorganization energy, the standard value of $\lambda = 35/\mathrm{cm}$ is employed. Along the lines of the discussion in [22], the standard bath correlation time is taken from 50 fs to 150 fs. We assume ambient temperature $T = 288\ \mathrm{K}\ (= 200/\mathrm{cm})$. The main results use 40 tiers (819 ADOs), and Eq. (4) is integrated up to maximally 20 ps.

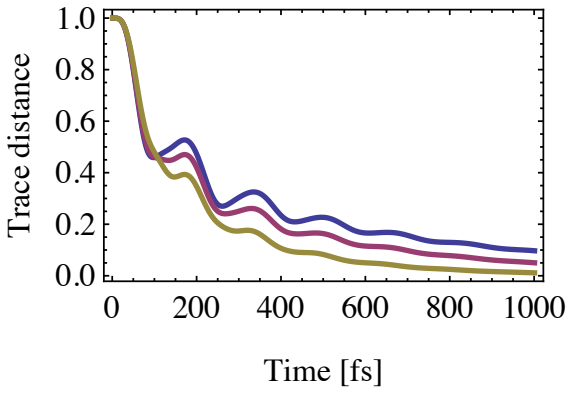

FIG. 1: Trace distance of the states $\rho_1 = |1\rangle\langle 1|$ and $\rho_2 = |2\rangle\langle 2|$ as a function of time for a two-site system (dimer) in the hierarchy equation of motion model. The trace distance evolves from maximally distinguishable $(= 1)$ for the initial states to zero for the thermal equilibrium state. At intermediate times, the trace distance increases, which is due a reversal of the information flow. Various bath correlation times are shown, 150 fs (blue), 100 fs (red), and 50 fs (yellow). For long correlation times, that is, a bath with more memory, the regions of positive slope of the trace distance are more pronounced.

First, in Fig 1, we investigate the time evolution of the trace distance in Eq. (1) for the dimer system. We choose the two initial states $\rho_1 = |1\rangle\langle 1|$ and $\rho_2 = |2\rangle\langle 2|$ and the standard parameters given above, while varying the bath dissipation rate. One can see clear non-Markovian revivals in the time intervals at around 150 fs and around 300 fs, borne out by increases in the trace distance. For larger correlation time of the bath of $\tau_c = 150$ fs these revivals are more pronounced. A bath excitation is more likely to return to the system instead of being dissipated away rapidly, as occurs in the case of smaller correlation time $\tau_c = 50$ fs.

The NM-ity measure involves an optimization of the initial states. On the one hand, the following results use the two initial states $\rho_1 = |1\rangle\langle 1|$ and $\rho_2 = |2\rangle\langle 2|$ as above but, one the other hand, compare to a systematically optimized pair of initial states. One initial state is chosen out of 50 pure states on the Bloch sphere. This leads to a total number of 1225 independent pairs of states in the optimization. (The state optimization itself is done with 20 tiers of ADOs.)

We now proceed to scan over the parameters of the model, beginning with the system parameters, the site energy difference and the chromophoric coupling. First, the NM-ity is strongly dependent on the chromophoric coupling, see Fig. 2 (a). At zero coupling, the molecules are independent and the

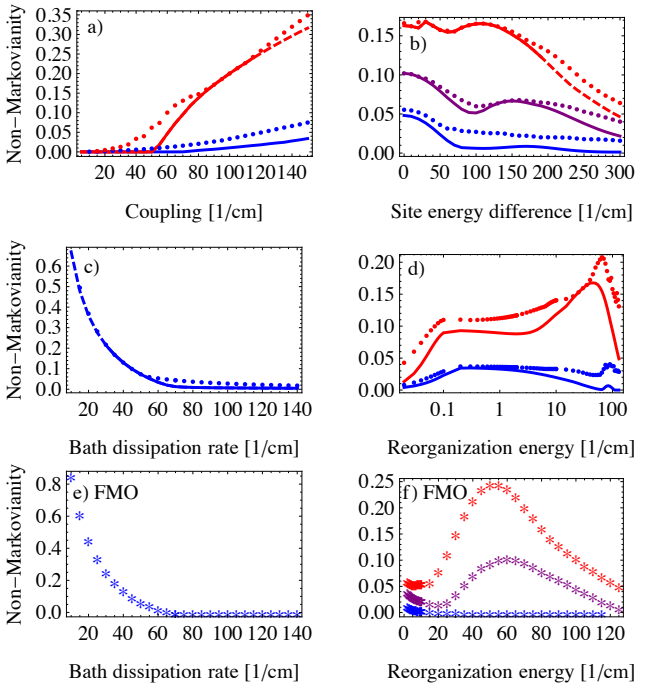

FIG. 2: Non-Markovianity as a function of the parameters of a dimer system, a)-d), and the Fenna-Matthews-Olson complex, e) and f), in the hierarchy equation of motion approach. For the dimer: a) coupling J_{12}, b) site energy difference $\epsilon_2 - \epsilon_1$, c) bath dissipation rate γ, and d) reorganization energy λ. The solid lines are calculations done with the initial states being $\rho_1 = |1\rangle\langle 1|$ and $\rho_2 = |2\rangle\langle 2|$ while the dots are computations done with optimized initial states. The dashed part of the lines indicates that the a respective parameter was scanned beyond the validity of the model based on the truncation condition. For the FMO complex: e) bath dissipation rate and f) reorganization energy. In all figures, except in c) and e), we use the different bath correlation times: 50 fs (blue), 100 fs (purple), and 150 fs (red).

NM-ity is zero; the two initial states remain perfectly distinguishable. At non-zero coupling, the dynamics shows increasing NM revivals, while both initial states converge to the same thermal equilibrium state. Second, with respect to the site energy difference, the dependence of the NM-ity weakly slopes downward, see Fig 2 (b). As the energy difference increases the coupling becomes less significant and the molecules become more independent. This leads to decreased NM-ity.

Next, we investigate the role of the bath parameters. First, as mentioned before, the bath correlation time crucially affects the memory of the bath and the information back flow to the system. In Fig. 2 (c), we show the NM-ity measure as a function of the inverse bath correlation time, i.e. the bath dissipation rate. A longer τ_c leads to more non-Markovianity, because a sluggish bath keeps the memory of excitations much longer and the information is able to return back to the electronic degrees of freedom. Second, the other significant bath parameter, the reorganization energy, is a measure of the non-equilibrium character of the phonon bath in the excited state. In Fig. 2 (d), we show the NM measure as a function of the reorganization energy. At zero λ, which essentially means no coupling to the phonons, the dynamics obviously shows zero non-Markovianity. At weak λ, we observe a NM-ity of around 0.1 at $t_c = 150$ fs, which is completely neglected by Redfield theory. At intermediate λ of around $40/\text{cm}$, close to the physiological values of the Fenna-Matthews-Olson complex, the NM-ity is maximal, showing a value of around 0.2. At large λ, the regime of incoherent transport [23], the NM-ity vanishes.

Results for the Fenna-Matthews-Olson complex– We now study the exciton-phonon information flow in the Fenna-Matthews-Olson complex. The FMO complex is found in green sulphur bacteria, where it connects the antenna complex with the reaction center. It is a trimer with seven bacteriochlorophyll (BChl) molecules in each subunit and with one additional BChl molecule shared between the units. We implement the hierarchy equation of motion for the seven sites ($N = 7$), using a method for rescaling the auxiliary systems as in [29]. Redefining the ADOs as $\tilde{\sigma}^{\mathbf{n}}(t) = \left(\prod_i n_i |c_0|^{-n_i}\right)^{-1/2} \sigma^{\mathbf{n}}(t)$ and rescaling the superoperators as $\phi_i \sigma^{\mathbf{n}_{i+1}} = \sqrt{(n_i+1)|c_0|}\phi_i \tilde{\sigma}^{\mathbf{n}_{i+1}}$ and $n_i \theta_i \sigma^{\mathbf{n}_{i-1}} = \sqrt{n_i/|c_0|}\theta_i \tilde{\sigma}^{\mathbf{n}_{i-1}}$, with $c_0 = \left(2\lambda\beta/\hbar^2 - i\lambda\gamma\right)$ in the high temperature regime, leads to a more balanced EOM and thus a lower requirement in terms of the number of ADOs. As was shown recently [30], with four tiers (329 ADOs) the coherent population dynamics can be accurately simulated, but due to the reduced number of ADOs, we expect to modestly overestimate the NM-ity. We use the initial states $\rho_1 = |1\rangle\langle 1|$ and $\rho_2 = |2\rangle\langle 2|$. First, the scan of γ obtains a strong dependence similar to the dimer system, see Fig. 2 (e). The NM-ity measure is 0.2 at $\tau_c = 150$ fs. Second, the scan of the reorganization energy obtains a maximum at around $\lambda = 55/\text{cm}$ with the NM-ity being 0.19 at $\lambda = 35/\text{cm}$ and $\tau_c = 150$ fs, see Fig. 2 (f). The results suggest that non-Markovian effects should play a significant role in the function of the Fenna-Matthews-Olson complex.

Experimental characterization– In principle, the recently proposed ultrafast quantum process tomography protocol extracts a full characterization of the quantum map [31], and could thus be used to determine information about the vibrational environment experimentally. Experiments specifically designed to extract a particular observable, such as in our case the NM-ity measure, could be done with a smaller number of experimental configurations. We provide a first step towards a resource efficient characterization of non-Markvianity and focus on the optimization of the non-Markovianity as a function of relevant experimental input parameters. Experiments on photosynthetic complexes are usually realized with ultrafast four-wave mixing to monitor excited state dynamics. The setup consists of three incoming laser pulses and one phase-matched outgoing pulse (which interferes with a local oscillator). The first two pulses at times t_1 and t_2, separated by the controllable coherence time $t_{\text{coh}} = t_2 - t_1$, prepare the initial state in the single exciton manifold while the third pulse at t_3 probes the time-evolved state after a time interval called the

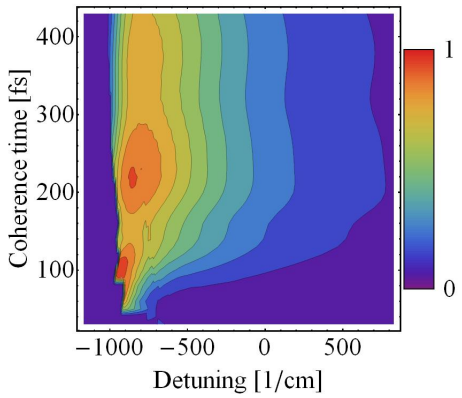

FIG. 3: Scan of the non-Markovianity during the population time (1 ps) of a simulated ultrafast experiment for a dimer system. The normalized quantity NM-ity$_{\rm exp}$/NM-ity$_{\rm exp}^{\rm max}$ is shown as a function of the detuning $\Omega - \Omega_{\rm ref}$ and the coherence time $t_{\rm coh}$. The maximum is observed at $\Omega - \Omega_{\rm ref} = -950/\text{cm}$ and $t_{\rm coh} = 100$ fs.

population time $t_{\rm pop} = t_3 - t_2$. We use the direct simulation method in [32, 33], including the rotating wave approximation. The excited state dynamics is governed by the hierarchy equation of motion, as before. The system parameters are again inspired by the site 1 and 2 dimer of the Fenna-Matthews-Olson complex with $\lambda = 35/\text{cm}$ and an intermediate bath correlation time $\tau_c = 100$ fs.

We study the NM-ity during the population time as a function of two basic parameters that play a crucial role in determining the initial state: the coherence time $t_{\rm coh}$ and the color of the laser pulses [4, 32, 33]. The Hamiltonian for the light-matter interaction is given by $H_{L-M} = \vec{E}(t)\,\vec{\mu}$, where the electric field is $\vec{E}(t) = \vec{\epsilon} A(t) e^{i\Omega t} + cc.$, with the amplitude $A(t)$, polarization $\vec{\epsilon}$, and the frequency Ω. The dipole moment is given by $\vec{\mu} = \sum_m \vec{\mu}_m \left(|0\rangle\langle m| + |m\rangle\langle 0|\right)$. We assume that the effective dipoles are $\vec{\mu}_{1/2}\vec{\epsilon} = 1$ [32, 33]. The weak Gaussian pulses have a standard deviation of 5 fs and an amplitude of $100/\text{cm}$. The experimentally relevant non-Markovianity during the population time is schematically determined by NM-ity$_{\rm exp}(\Omega, t_{\rm coh}) = \int_{t_2}^{t_2+t_{\rm pop}} dt\ \alpha(\sigma(t))\,\sigma(\rho_{\Omega,t_{\rm coh}}(t), \rho_{\rm ref}(t))$, which is investigated in Fig. 3. Here, $t_{\rm pop} = 1$ ps and $\rho_{\rm ref}$ is a reference state with $\Omega_{\rm ref} = 12370/\text{cm}$ (centered at the higher exciton frequency) and $t_{\rm coh,ref} = 30$ fs (to avoid pulse overlap effects). The maximal value is given by NM-ity$_{\rm exp}^{\rm max} = \max_{\Omega,t_{\rm coh}}$NM-ity$_{\rm exp}(\Omega, t_{\rm coh})$. The maximum is observed at a detuning $\Omega - \Omega_{\rm ref}$ of around $-950/\text{cm}$ and at a $t_{\rm coh} = 100$ fs (and a second maximum is at around $-850/\text{cm}$ and 220 fs). The optimal pulses create an initial state as different as possible from $\rho_{\rm ref}$ in terms of NM-ity, with a detuning that leads to enough frequency overlap to populate the excited states and with a $t_{\rm coh}$ that harnesses the time evolution between the two state-preparation pulses.

Conclusion– We have shown numerically that there is a considerable non-Markovian information flow between electronic and phononic degrees of freedom of light-harvesting chromophoric systems under physiological conditions, utilizing a realistic model for systems such as the Fenna-Matthews-Olson complex. The results suggest that non-Markovianity plays a significant role in photosynthetic energy transfer. We have provided a first step towards the experimental quantification of non-Markovianity by studying a class of initial states obtained in a four-wave mixing experiment. Future work will investigate analytically and numerically how to efficiently extract the non-Markovianity from the phase-matched signal.

The authors are grateful to J. Piilo, C. Rodriguez-Rosario, and J. Zhu for insightful discussions. This material is based upon work supported as a part of the Center for Excitonics, as an Energy Frontier Research Center funded by the U.S. Department of Energy, Office of Science, Office of Basic Energy Sciences under Award number de-sc0001088. A. A.-G. acknowledges support from the Defense Advanced Research Projects Agency grant entitled "Room Temperature Coherent Energy Transfer: New Routes to Biomimetic Devices" through the Quantum Effects in Biological Environments program, award number N66001-10-1-4060. We acknowledge Harvard Research Computing for computational resources.

* Electronic address: rebentr@fas.harvard.edu
† Electronic address: aspuru@chemistry.harvard.edu

[1] R. E. Blankenship, *Molecular Mechanisms of Photosynthesis* (Wiley-Blackwell, 2002), 1st ed.
[2] Y.-C. Cheng and G. R. Fleming, Annual Review of Physical Chemistry **60**, 241 (2009).
[3] G. S. Engel, T. R. Calhoun, E. L. Read, T.-K. Ahn, T. Mancal, Y.-C. Cheng, R. E. Blankenship, and G. R. Fleming, Nature **446**, 782 (2007).
[4] H. Lee, Y.-C. Cheng, and G. R. Fleming, Science (New York, N.Y.) **316**, 1462 (2007).
[5] G. Panitchayangkoon, D. Hayes, K. A. Fransted, J. R. Caram, E. Harel, J. Wen, R. E. Blankenship, and G. S. Engel, Proceedings of the National Academy of Sciences p. 1 (2010).
[6] E. Collini, C. Y. Wong, K. E. Wilk, P. M. G. Curmi, P. Brumer, and G. D. Scholes, Nature **463**, 644 (2010).
[7] M. Mohseni, P. Rebentrost, S. Lloyd, and A. Aspuru-Guzik, The Journal of Chemical Physics **129**, 174106 (2008).
[8] P. Rebentrost, M. Mohseni, I. Kassal, S. Lloyd, and A. Aspuru-Guzik, New Journal of Physics **11**, 033003 (2009).
[9] M. B. Plenio and S. F. Huelga, New Journal of Physics **10**, 113019 (2008).
[10] J. Wu, F. Liu, Y. Shen, J. Cao, and R. J. Silbey, http://arxiv.org/abs/1008.2236 (2010).
[11] O. Mülken and T. Schmid, Physical Review E **82** (2010).
[12] M. Sarovar, A. Ishizaki, G. R. Fleming, and K. B. Whaley, Nature Physics **6**, 462 (2010).
[13] F. Fassioli and A. Olaya-Castro, http://arxiv.org/abs/1003.3610 (2010).
[14] F. Caruso, A. Chin, A. Datta, S. Huelga, and M. Plenio, Physical Review A **81**, 1 (2010).
[15] S. Jang, Y.-C. Cheng, D. R. Reichman, and J. D. Eaves, The Journal of Chemical Physics **129**, 101104 (2008).
[16] J. Roden, A. Eisfeld, W. Wolff, and W. Strunz, Physical Review

Letters **103**, 3 (2009).
[17] J. Piilo, S. Maniscalco, K. Härkönen, and K.-A. Suominen, Physical Review Letters **100**, 1 (2008).
[18] P. Rebentrost, R. Chakraborty, and A. Aspuru-Guzik, The Journal of Chemical Physics **131**, 184102 (2009).
[19] M. Thorwart, J. Eckel, J. Reina, P. Nalbach, and S. Weiss, Chemical Physics Letters **478**, 234 (2009).
[20] J. Prior, A. Chin, S. Huelga, and M. Plenio, Physical Review Letters **105**, 1 (2010).
[21] A. Ishizaki and G. R. Fleming, The Journal of Chemical Physics **130**, 234110 (2009).
[22] A. Ishizaki and G. R. Fleming, Proceedings of the National Academy of Sciences of the United States of America **106**, 17255 (2009).
[23] A. Ishizaki and G. R. Fleming, The Journal of Chemical Physics **130**, 234111 (2009).
[24] A. K. Rajagopal, A. R. U. Devi, and R. W. Rendell, http://arxiv.org/abs/1007.4498 (2010).
[25] H.-P. Breuer, E.-M. Laine, and J. Piilo, Physical Review Letters **103**, 1 (2009).
[26] M. Wolf, J. Eisert, T. Cubitt, and J. Cirac, Physical Review Letters **101**, 1 (2008).
[27] A. Rivas, S. Huelga, and M. Plenio, Physical Review Letters **105**, 1 (2010).
[28] M. A. Nielsen and I. L. Chuang, *Quantum Computation and Quantum Information* (Cambridge University Press, 2000), 1st ed.
[29] Q. Shi, L. Chen, G. Nan, R.-X. Xu, and Y. Yan, The Journal of Chemical Physics **130**, 084105 (2009).
[30] J. Zhu, S. Kais, P. Rebentrost, and A. Aspuru-Guzik, submitted (2010).
[31] J. Yuen-Zhou, M. Mohseni, and A. Aspuru-Guzik, http://arxiv.org/abs/1006.4866 (2010).
[32] T. Mancal, A. V. Pisliakov, and G. R. Fleming, The Journal of Chemical Physics **124**, 234504 (2006).
[33] A. V. Pisliakov, T. Mancal, and G. R. Fleming, The Journal of Chemical Physics **124**, 234505 (2006).